Electronic Supplementary Material (ESI) for Environmental Science: Nano.

Supplementary Information

Simultaneous sensitive detection and rapid adsorption of UO_2^{2+} based on post-modified *sp*^{2} carbon conjugated covalent organic framework

Cheng-Rong Zhang,[1] Wei-Rong Cui,[1] Wei Jiang,[1] Fang-Fang Li,[1] Yi-Di Wu,[1] Ru-Ping Liang,[1] Jian-Ding Qiu[1,2]*

[1]College of Chemistry, Nanchang University, Nanchang 330031, China

[2]Engineering Technology Research Center for Environmental Protection Materials and Equipment of Jiangxi Province, Pingxiang University, Pingxiang 337055, China

*Corresponding authors. Tel/Fax: +86-791-83969518. E-mail: jdqiu@ncu.edu.cn.

Contents

Chemicals. 2,4,6-tris(4-formylphenyl)-1,3,5-triazine (TFPT) and 2,4,6-triformylphloroglucinol (PDAN), were purchased from Chinese Academy of Sciences-Yanshen Technology Co.,Ltd. $UO(NO_3)_2$ and caesium carbonate (Cs_2CO_3) were available from Sigma-Aldrich. 1,4-dioxane, acetone, N,N-dimethylformamide (DMF), hydrochloric acid, sodium hydroxide, mesitylene, citric acid ($C_6H_8O_7$), ethanol, tetrahydrofuran (THF) and other nitrate salts (Cd^{2+}, Na^+, Cu^{2+}, Zn^{2+}, Ni^{2+}, Mn^{2+}, Fe^{3+}, Cr^{3+}, Co^{2+}, K^+, Ca^{2+}, Mg^{2+}, Al^{3+}, Ba^{2+}, Sr^{2+}, Cs^+, Pb^{2+}, Eu^{3+}, Sm^{3+}, La^{3+}, VO_4^{3-}) were purchased from Sinopharm Chemical Reagent Co, Ltd. All reagents used were not further purification and ultrapure water (18.2 MΩ) was applied as experiments water from a Millipore Milli-Q system. All reagents, unless otherwise noted, were purchased from commercial sources and used without further purification.

Instrument. FT-IR spectra were recorded with a Bruker TENSOR 27 instrument. Powder X-ray diffraction (PXRD) data of the nanomaterials were collected on a Bruker AXS D8 Advance A25 Powder X-ray diffractometer (40 kV, 40 mA) using Cu Kα (λ=1.5406 Å) radiation. The fluorescence (FL) spectra were recorded on a FL spectrophotometer (F-7000, Hitachi). X-ray photoelectron spectroscopy (XPS) spectra were performed on a Thermo VG Multilab 2000X with Al Kα irradiation. The ^{13}C CP/MAS NMR spectra were recorded with a 4-mm double-resonance MAS probe and with a sample spinning rate of 10.0 kHz; a contact time of 2 ms (ramp 100) and a pulse delay of 3 s were applied. The nitrogen adsorption and desorption isotherms were measured at 77 K using a Micromeritics ASAP 2020M system. All the COF samples were outgassed for 12 h at 150 °C under vacuum prior to the gas adsorption studies. The surface areas were evaluated using Brunauer-Emmett-Teller (BET) model applied between P/P_0 values of 0.05 and 1.0 for mesoporous COF. The pore size distributions were calculated using the non-localized density functional theory (NLDFT) method. The thermal properties of the nanomaterials were evaluated using a STA PT1600 Linseis thermogravimetric analysis (TGA) instrument over the temperature range of 30 to 800 °C under nitrogen atmosphere with a heating rate of 10 °C/min. Inductively coupled plasma-mass spectrometry (ICP-MS) was used to determine the concentrations of UO_2^{2+}. Thermogravimetric analysis (TGA) was carried out utilizing a Germany Benz TG 209F. The solid-state nuclear magnetic resonance spectrum (Agilent Technologies, Santa Clara, CA, USA) was performed on an Agilent-NMR-Vnmrs 600 spectrometer. N_2 adsorption-desorption isotherms were measured on 77 K by Micromeritics TriStar II 3020 analyzer.

Preparation of uranium and metal ions stock solution. A stock solution of uranyl nitrate (~1000 mg L^{-1}) was prepared by dissolving appropriate amounts of $UO_2(NO_3)_2{\cdot}6H_2O$ in a suitable amount of concentrated nitric acid solution and the pure uranium working solutions (15-300 mg L^{-1}) were prepared by appropriate dilution of the stock solution. The metal ions stock solutions (1 mM) were prepared by dissolving the nitrate salts including (Cd^{2+}, Na^{+}, Cu^{2+}, Zn^{2+}, Ni^{2+}, Mn^{2+}, Fe^{3+}, Cr^{3+}, Co^{2+}, K^{+}, Ca^{2+}, Mg^{2+}, Al^{3+}, Ba^{2+}, Sr^{2+}, Cs^{+}, Pb^{2+}, Eu^{3+}, Sm^{3+}, La^{3+}, VO_4^{3-}) in ultrapure water.

Synthesis of TP-COF. A 50 mL pyrex tube was charged with TFPT (42.5 mg, 0.108 mM), PDAN (25.46 mg, 0.163 mM), 1,4-dioxane (5 mL) and caesium carbonate (209 mg, 0.575 mM). This mixture was sonicated for 10 min, degassed through three freeze-pump-thaw cycles, sealed under vacuum, and heated at 120 °C for 3 days. The reaction mixture was cooled to room temperature and the precipitate was centrifuged and washed with H_2O, ethanol and THF several times, and dried under vacuum at 80 °C for 10 h to afford yellow powder in 86% isolated yield.

Synthesis of TP-COF-AO. Amidoxime functionalized COF (TP-COF-AO) was synthesized by treatment of TP-COF (250 mg) with $NH_2OH{\cdot}HCl$ (470 mg) and triethylamine (3 mL) in ethanol (65 mL) at 80 °C for 24 h. After the reaction, the mixture was cooled to room temperature and washed three times with deionized water and ethanol, and then dried at 80 °C under vacuum to obtain TP-COF-AO (230 mg) as pale yellow powder.

Synthesis of TP-POP. A 50 mL pyrex tube was charged with TFPT (42.5 mg, 0.108 mM), PDAN (25.46 mg, 0.163 mM), 1,4-dioxane (5 mL) and KOH (0.5 mL, 5 M). This mixture was sonicated for 10 min, degassed through three freeze-pump-thaw cycles, sealed under vacuum, and heated at 120 °C for 3 days. The reaction mixture was cooled to room temperature and the precipitate was centrifuged and washed with H_2O, ethanol and THF several times, and dried under vacuum at 80 °C for 10 h.

Synthesis of TP-POP-AO. The procedures for the synthesis of TP-POP-AO are similar to those of TP-COF-AO, except TP-POP is used instead of TP-COF.

Fluorescence detection of UO_2^{2+}. A stock solution of TP-COF-AO was prepared by dispersing TP-COF-AO in DMF. For the sensitivity tests, 2 mL of TP-COF-AO stock solution (0.02 mg/mL) was placed in a 4 mL quartz cuvette, then added different concentrations of UO_2^{2+} (pH=6) and recorded the fluorescence spectra immediately. In the selective experiment 50 μM other ions (Cd^{2+}, Na^{+}, Cu^{2+}, Zn^{2+}, Ni^{2+}, Mn^{2+}, Fe^{3+}, Cr^{3+}, Co^{2+}, K^{+}, Ca^{2+}, Mg^{2+}, Al^{3+}, Ba^{2+}, Sr^{2+}, Cs^{+}, Pb^{2+}, Eu^{3+}, Sm^{3+}, La^{3+}, VO_4^{3-}, and mixed ions) were added to TP-COF-AO stock solution (0.02 mg/mL) and then recorded fluorescence changes immediately and taken photos with a Nikon j5 digital camera. All the measurements, unless otherwise noted, were excited at λ_{ex} = 280 nm and the corresponding emission wavelength was tested from λ_{em} = 300 to 650 nm, each test was repeated at least for three times. Unless otherwise stated, all measurements are taken in DMF.

Recycle studies. For the recycle tests, 2 mL of TP-COF-AO stock solution (0.02 mg/mL) in a quartz cuvette, the fluorescence spectra were measured before and after the stock UO_2^{2+} solution (20 μM) was added. The stock solution of 1 M Na_2CO_3 were further added to remove UO_2^{2+} from TP-COF-AO@UO_2^{2+}, and the recycled TP-COF-AO was reused in the next UO_2^{2+} detection and removal. The measured fluorescence intensities were used to assess the degree of the recovery.

Removal of UO_2^{2+} by TP-COF-AO. The aqueous solutions of uranium with different concentrations were obtained by diluting the stock metal solution with the proper amount of distilled water unless otherwise indicated. The pH values of the solutions were adjusted by HNO_3 or NaOH aqueous solution. The concentrations of uranium during all the experiments were detected by inductively coupled plasma-mass spectrometry (ICP-MS) for extra low concentrations. All the adsorption experiments were performed at ambient conditions. A sample of uranium solution without sorbent material was analyzed for each sorption experiment as a negative control.

To obtain the uranium adsorption isotherms for TP-COF-AO (5 mg) were added into 10 mL aqueous solutions with different concentrations of uranium. Adsorbents were suspended fully by brief sonication and then the mixtures were stirred vigorously overnight, by which time it was assumed that adsorption equilibrium had been reached. The treated solutions were filtered through a 0.22 μm membrane filter. The supernatant was analyzed using ICP analysis to determine the remaining uranium concentration. The adsorbed amount at equilibrium (q_e, mg g^{-1}) was calculated by

$$q_e = \frac{(C_0 - C_e) \times V}{m}$$

q_e is adsorption capacity (mg/g), C_0 and C_e are the initial concentration of UO_2^{2+} and the final UO_2^{2+} concentration (mg L^{-1}), respectively, V is the volume of the UO_2^{2+} solution (L), m is the the amount of used adsorbent (g).

Uranium sorption kinetics from distilled water uranium aqueous solution (20 mL, 9.25 ppm), and adsorbent (5 mg) were added to glass vials. The mixture was shaken at room temperature for 3 h. At appropriate time intervals, aliquots were taken from the mixture, and the adsorbents were separated by a syringe filter (0.22 μm membrane filter). The uranium concentrations in the resulting solutions were analyzed by ICP-MS. The adsorption capacity at different intervals was calculated as follows:

$$q_t = \frac{C_0 - C_t}{m} \times V$$

q_t is adsorption capacity (mg/g), C_O and C_t are the initial concentration of UO_2^{2+} and the UO_2^{2+} concentration at time t (mg L^{-1}), respectively, V is the volume of the UO_2^{2+} solution (L), m is the the amount of used adsorbent (g).

Uranium removal kinetics from water, uranium spiked water samples (100 mL, 9.25 ppm) and adsorbents (5 mg) were added to an Erlenmeyer flask with a magnetic stir bar. The mixture was stirred at room temperature. At appropriate time intervals, aliquots (5 mL) were taken from the mixture, and the adsorbents were separated by a syringe filter (0.22 μm membrane filter). The uranium concentrations in the resulting solutions were analyzed by ICP-MS. The percentage removal of uranium species was calculated as follows:

$$\text{Removal percentage} = \frac{C_0 - C_e}{C_0} \times 100\%$$

The partition coefficient K_d is an valuable parameter for determining the affinity and selectivity performance of the adsorbent for UO_2^{2+}, which can be determined by formula:

$$K_d = \frac{C_0 - C_e}{C_e} \times \frac{V}{m}$$

The experimental results were fitted using the pseudo-second-order kinetic model by the equation (4):

$$\frac{t}{q_t} = \frac{1}{k_2 q_e{}^2} + \frac{t}{q_e}$$

k^2 (g mg^{-1} min^{-1}) is the rate constant of pseudo-second-order adsorption model, and q_e (mg g^{-1}) is the amount of $UO_2{}^{2+}$ adsorbed at equilibrium.

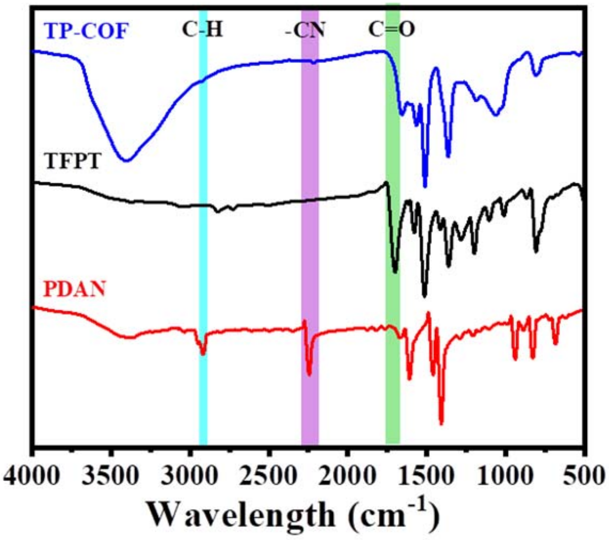

Fig. S1. FT-IR spectra of TP-COF, TFPT and PDAN.

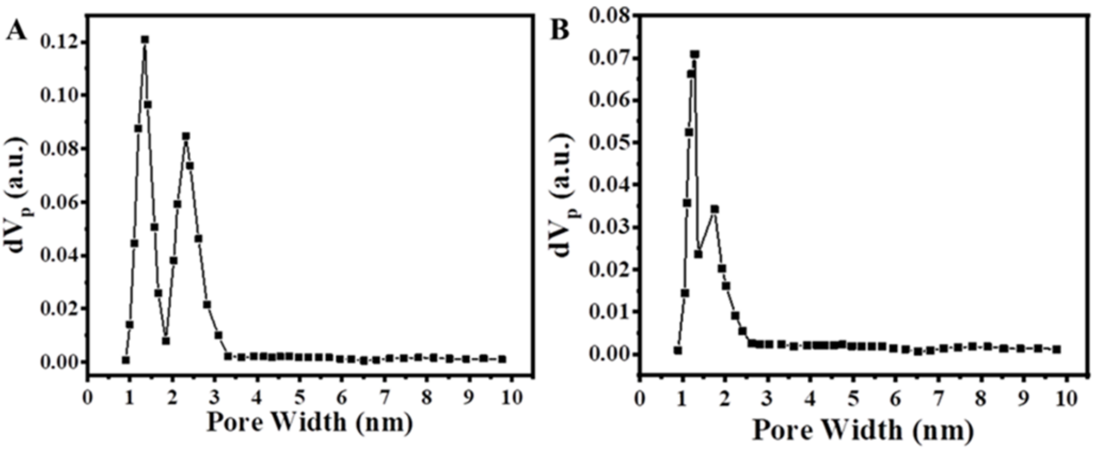

Fig. S2. Pore size distributions of TP-COF (A) and TP-COF-AO (B).

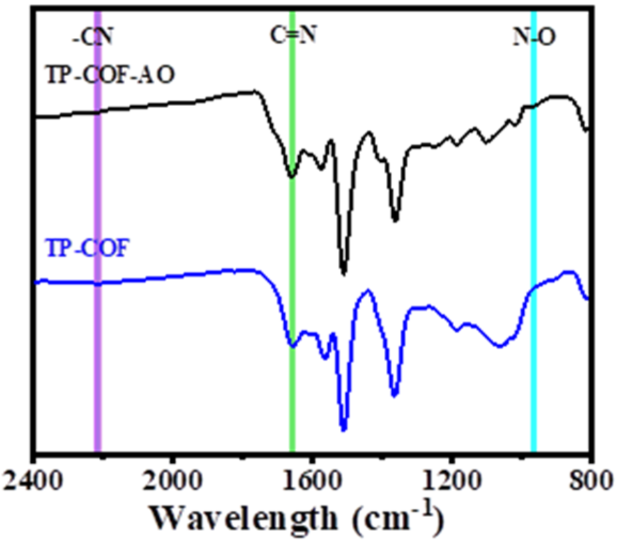

Fig. S3. FT-IR spectra of TP-COF and TP-COF-AO.

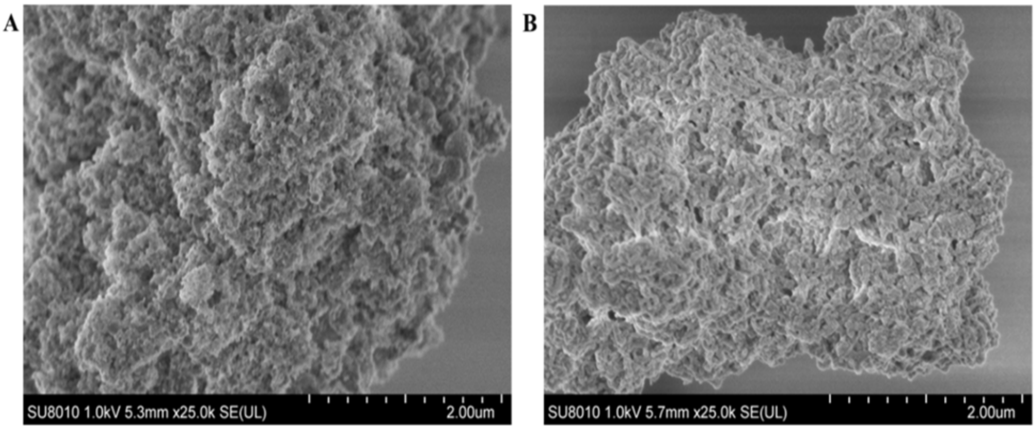

Fig. S4. SEM images of TP-COF (A), TP-COF-AO (B).

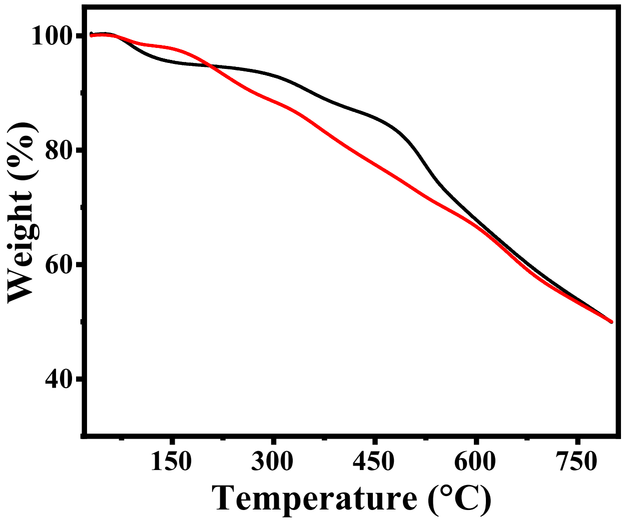

Fig. S5. TGA curves of the TP-COF (black) and TP-COF-AO (red).

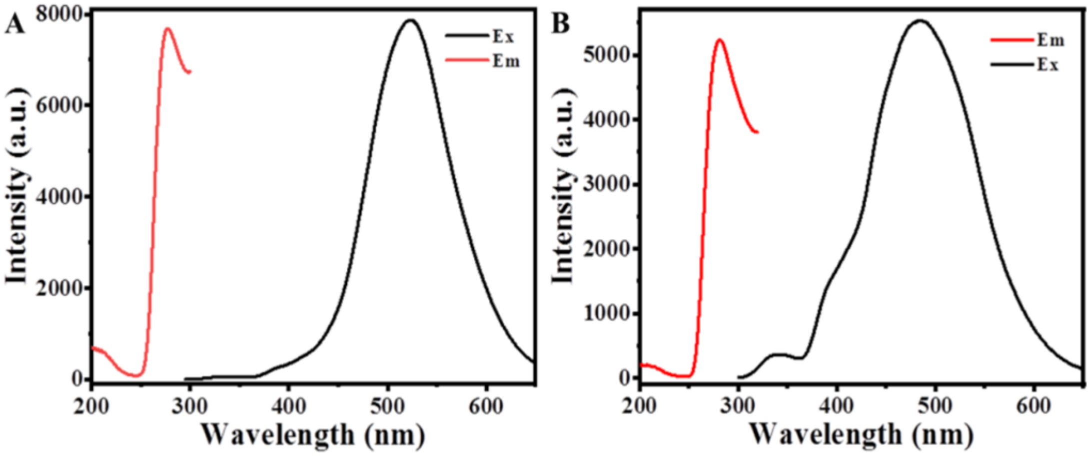

Fig. S6. Normalized fluorescence excitation (red) and emission (black) spectra of TP-COF (A) and TP-COF-AO (B) dispersed in DMF.

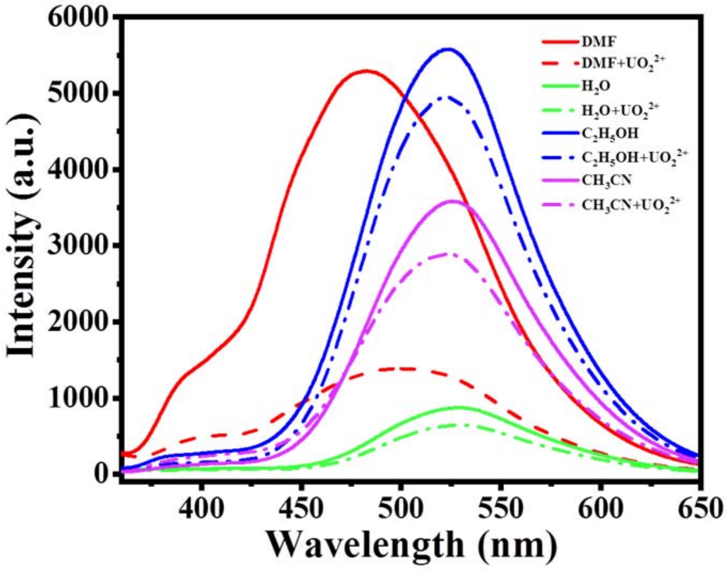

Fig. S7. Fluorescence spectra of TP-COF-AO dispersed in H_2O (green), C_2H_5OH (green), DMF (red), and CH_3CN (blue) before (solid lines) and after (dashed lines) the addition of UO_2^{2+} (20 μM) ($\lambda_{ex} = 280$ nm).

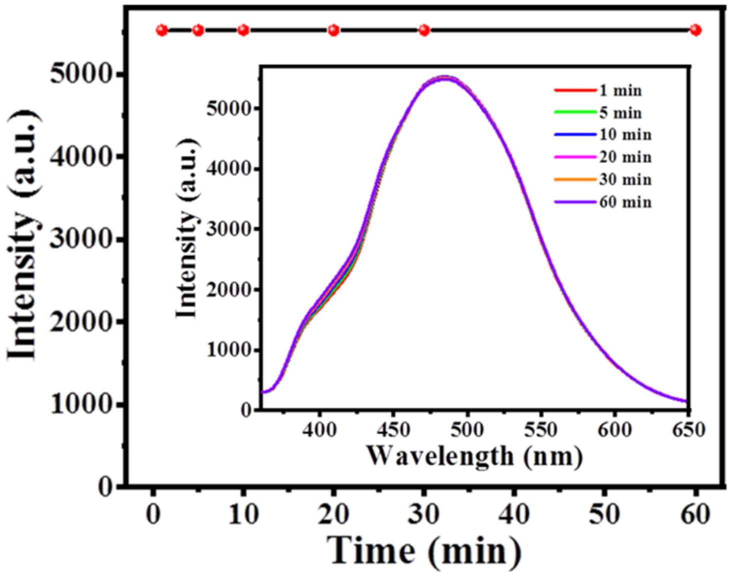

Fig. S8. Time-dependent fluorescence intensity of TP-COF-AO tested within 60 minutes. The unchanged intensity indicates that TP-COF-AO does not show any photo-bleaching, and the observed decrease in intensities in other cases is indeed induced by the addition of ions, such as UO_2^{2+}.

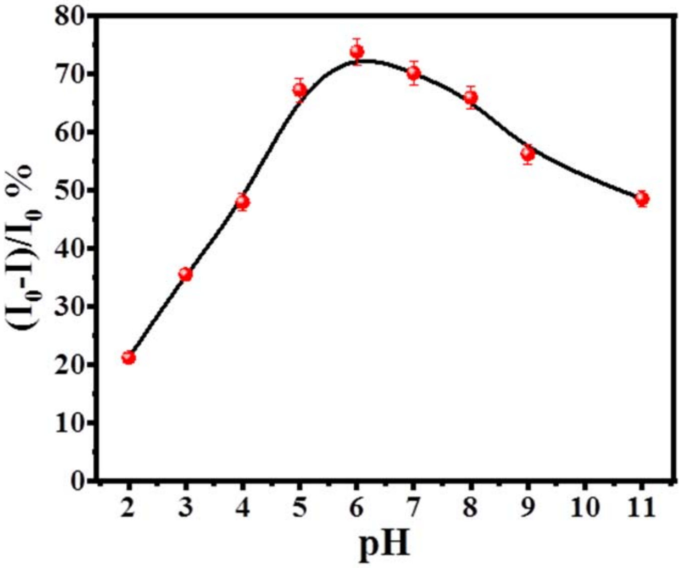

Fig. S9. The fluorescence quenching ratio $[(I_0\text{-}I)/I_0]$% of TP-COF-AO in the presence of 20 μM UO_2^{2+} at different pH.

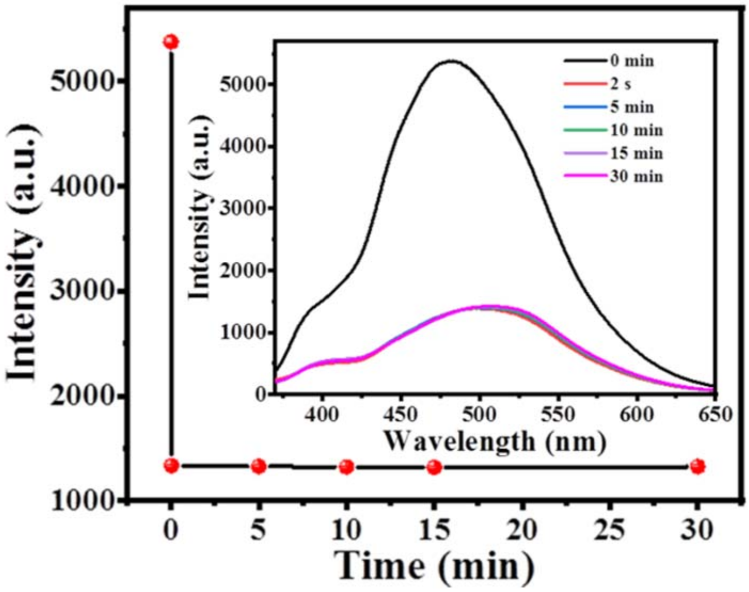

Fig. S10. TP-COF-AO after addition of UO_2^{2+} (20 μM) was tested within 30 minutes.

Table S1. Comparison of the equilibrium time for various methods for detecting uranium.

System	Detection method	Respond time	Ref
AuPd nanoalloy	Resonance scattering spectral	8 min	1
DNAzyme	Electrochemistry	10 min	8
Ag-rGO sheets	SERS	240 min	11
DNAzyme-AuNP	Colorimetric	30 min	4
OPA-Au NPs	Colorimetric	5 min	3
BSA-AuNCs	Colorimetric	30 min	9
Enzyme-free dual amplification	Colorimetric	10 min	7
T-PADAP	Colorimetric	10 min	10
HFSA	Fluorescence	10 min	5
G-quadruplex-assisted enzyme	Fluorescence	30 min	6
PCSA	Fluorescence	30 min	2
TP-COF-AO	Fluorescence	2 s	This work

Table S2. Comparison of the detection limit of uranium for various methods.

System	Detection method	Detection limit	Ref
T-PADAP	Colorimetric	4 M	4
DNAzyme	Colorimetric	13.7 nM	7
BSA-AuNCs	Colorimetric	1.86μM	9
RuNPs / GC	Electrochemistry	8.45 nM	14
DNAzyme	Fluorescence	0.41 nM	12
PCSA	Fluorescence	0.86 nM	2
HFSA	Fluorescence	2.1 nM	5
Zn(II)-MOF	Fluorescence	81 M	13
CDs/SBA-NH_2	Fluorescence	4.3 μM	15
ESF-1-Eu	Fluorescence	1.26 μM	16
TP-COF-AO	Fluorescence	8.3 nM	This work

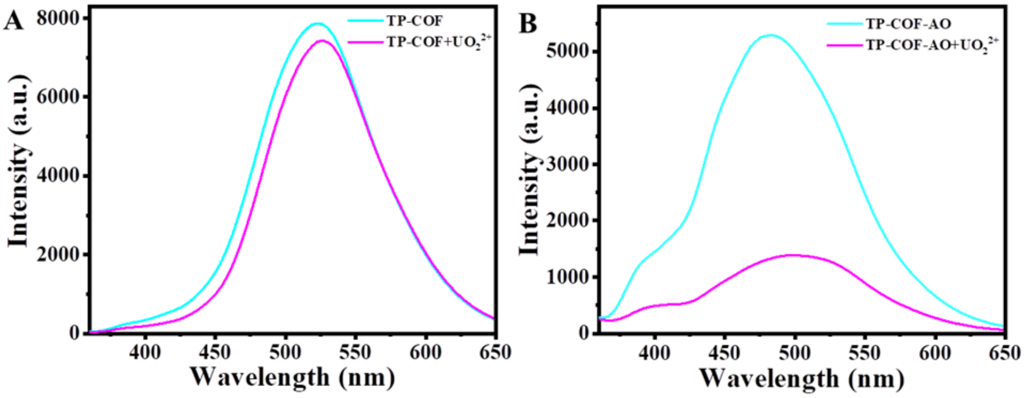

Fig. S11. Fuorescence emission spectra of TP-COF (A) and TP-COF-AO (B) before and after addition of UO_2^{2+} (20 μM).

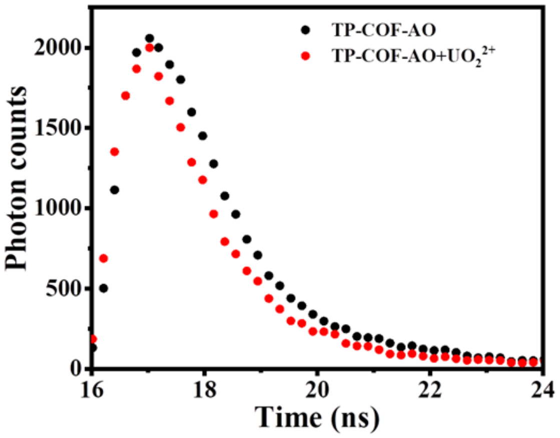

Fig. S12. Fluorescence decay curves of TP-COF-AO in the presence of UO_2^{2+}.

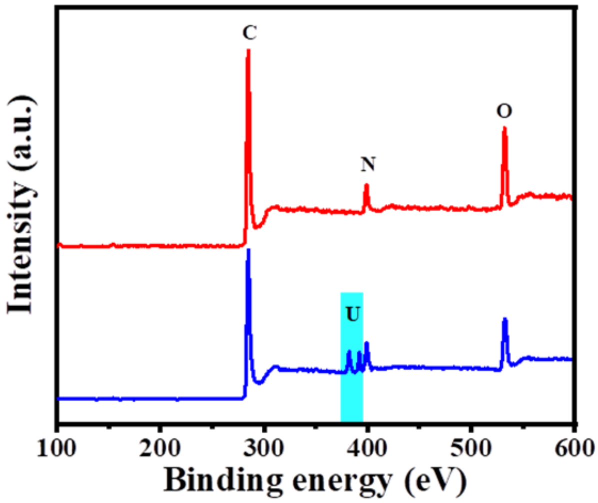

Fig. S13. XPS survey spectra of TP-COF-AO before (red) and after adsorption of UO_2^{2+} (blue).

Table S3. Comparison of the adsorption capacity for various adsorbents.

Adsorbents	**Adsorption capacity (mg g^{-1})**	**Ref**
MCM-41	58.9	17
Magnetic Schiff base	94.3	18
CMPAO	251.9	19
MA-TMA	1028	20
HTC-MA-TMA	271.83	21
PECQDs/ $MnFe_2O_4$	194.2	22
o-GS-COF	220	23
PAF-1-CH_2AO	283	24
C-HCN-AO	355.6	25
COF-TpDb-AO	408	26
TP-COF-AO	436	This work

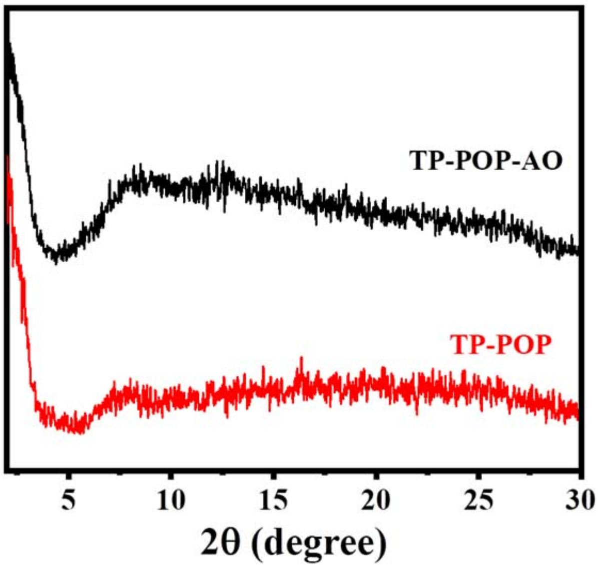

Fig. S14. XRD pattern of TP-POP and TP-POP-AO.

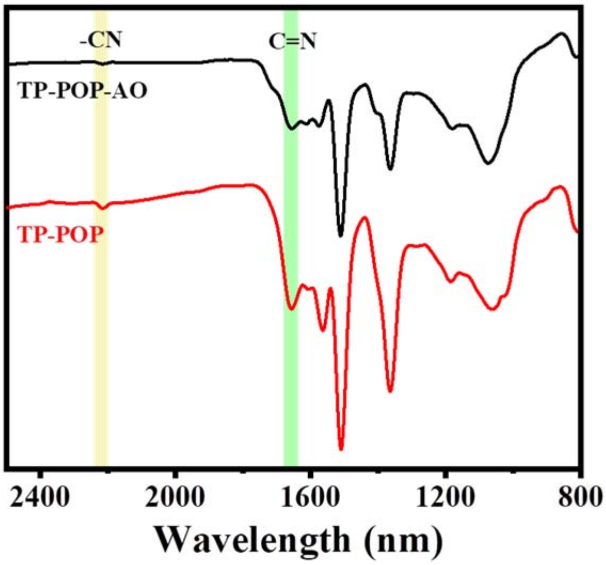

Fig. S15. FT-IR spectra of TP-POP and TP-POP-AO.

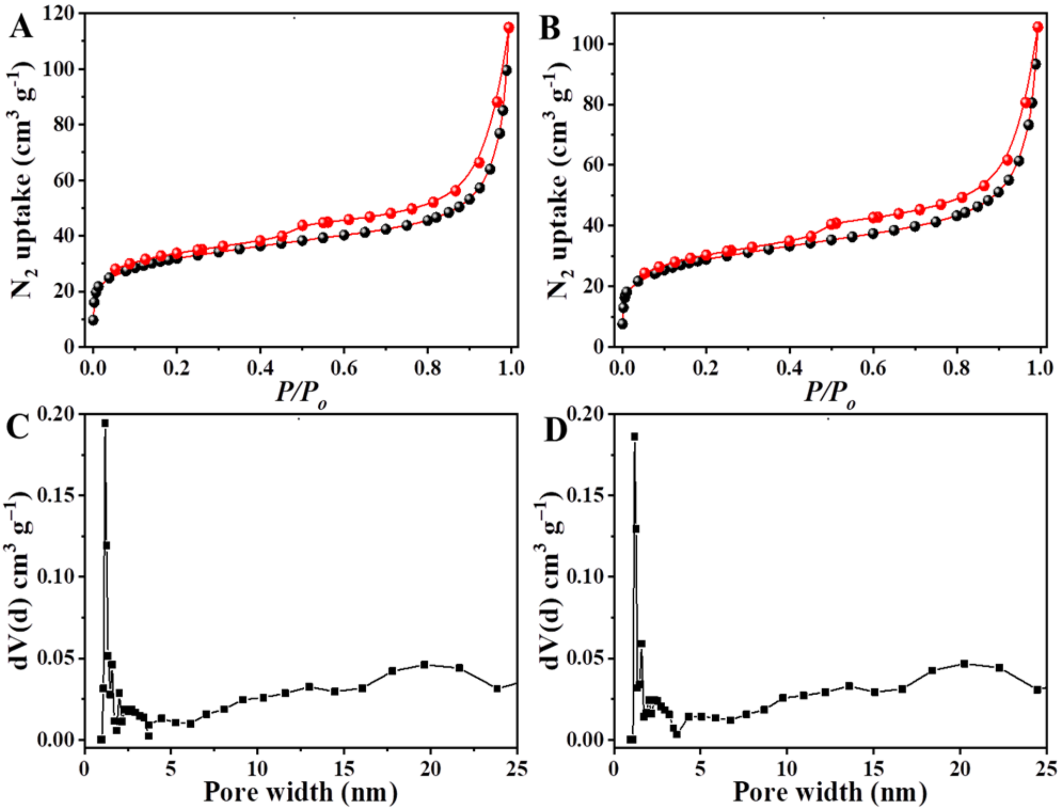

Fig. S16. Nitrogen-sorption isotherm curves measured at 77 K for TP-POP **(A)** and TP-POP-AO (B). Corresponding pore size distribution calculated based upon NLDFT of TP-POP (C) and TP-POP-AO (D). The BET surface area of TP-POP and TP-POP-AO were calculated to be 118 and 90 m^2 g^{-1}, respectively.

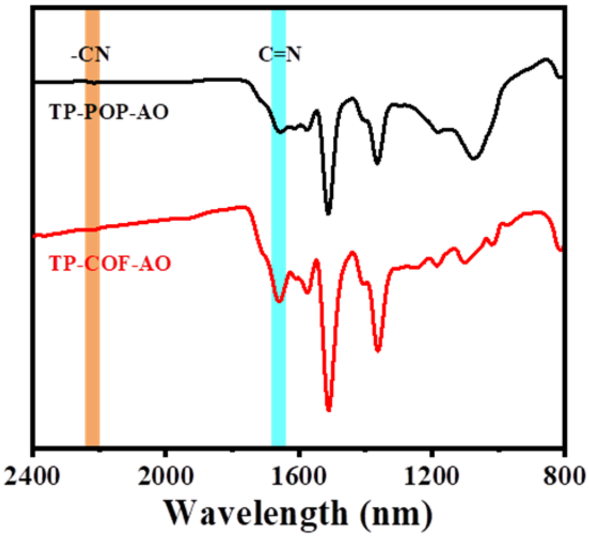

Fig. S17. FT-IR spectra of TP-COF-AO and TP-POP-AO.

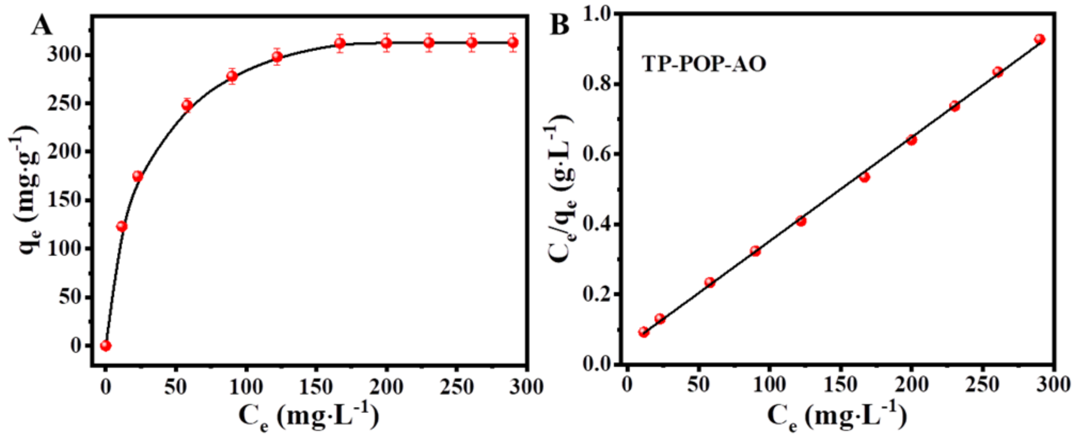

Fig. S18. (A) Adsorption isotherm of TP-POP-AO for UO_2^{2+}. (B) The linear regression by fitting the adsorption data with Langmuir adsorption model.

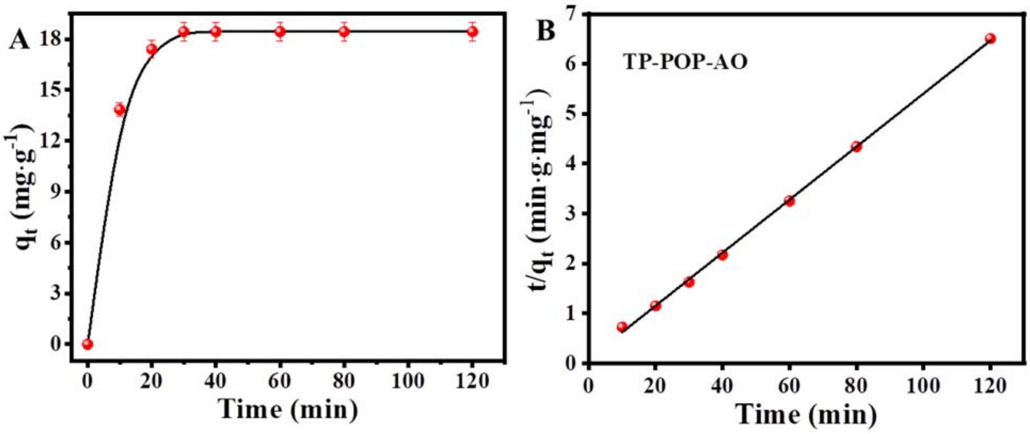

Fig. S19. (A) Adsorption curve of UO_2^{2+} versus contact time in water using TP-POP-AO. (B) The pseudo-second-order kinetic plot for the adsorption.

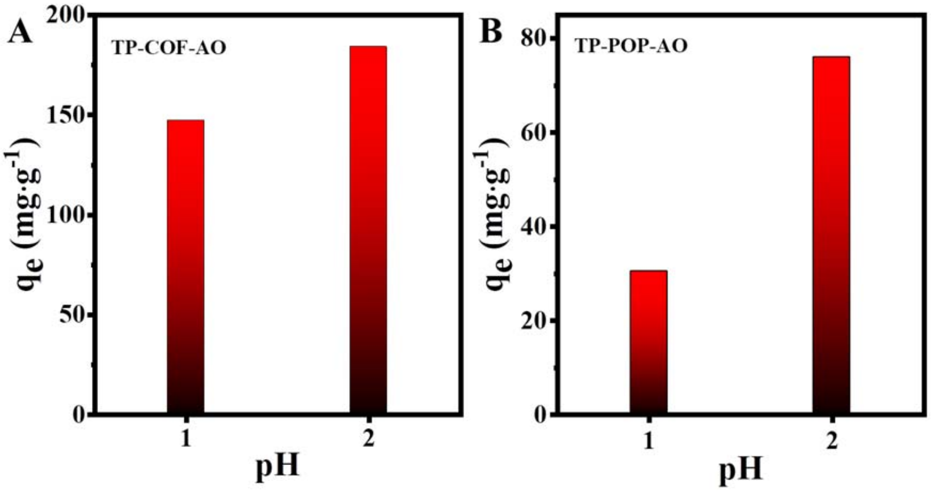

Fig. S20. The uranium adsorption capacities of TP-COF-AO (A) and TP-POP-AO (B) at pH 1.0 and pH 2.0.

References

1. A. Liang, Y. Zhang, Y. Fan, C. Chen, G. Wen, Q. Liu, C. Kang and Z. Jiang, Catalysis of aptamer-modified AuPd nanoalloy probe and its application to resonance scattering detection of trace UO_2^{2+}, *Nanoscale*, 2011, **3**, 3178-3184.
2. X. Chen, L. He, Y. Wang, B. Liu and Y. Tang, Trace analysis of uranyl ion (UO_2^{2+}) in aqueous solution by fluorescence turn-on detection via aggregation induced emission enhancement effect, *Anal. Chim. Acta*, 2014, **847**, 55-60.
3. X.-H. Cao, H.-Y. Zhang, R.-C. Ma, Q. Yang, Z.-B. Zhang and Y.-H. Liu, Visual colorimetric detection of UO_2^{2+} using o-phosphorylethanolamine-functionalized gold nanoparticles, *Sensor Actuat. B-chem*, 2015, **218**, 67-72.
4. J. H. Lee, Z. Wang, J. Liu and Y. Lu, Highly sensitive and selective colorimetric sensors for uranyl (UO_2^{2+}): development and comparison of labeled and label-free DNAzyme-goldnanoparticle systems, *J. Am. Chem. Soc.*, 2008, **130**, 14217-14226.
5. X. Chen, L. Peng, M. Feng, Y. Xiang, A. Tong, L. He, B. Liu and Y. Tang, An aggregation induced emission enhancement-based ratiometric fluorescent sensor for detecting trace uranyl ion (UO_2^{2+}) and the application in living cells imaging, *J. Lumin.*, 2017, **186**, 301-306.
6. P. Zhu, Y. Zhang, S. Xu and X. Zhang, G-quadruplex-assisted enzyme strand recycling for amplified label-free fluorescent detection of UO_2^{2+}, *Chin. Chem. Lett.*, 2019, **30**, 58-62.
7. C. Huang, X. Fan, Q. Yuan, X. Zhang, X. Hou and P. Wu, Colorimetric determination of uranyl (UO_2^{2+}) in seawater via DNAzyme-modulated photosensitization, *Talanta*, 2018, **185**, 258-263.
8. W. Yun, J. Jiang, D. Cai, X. Wang, G. Sang, J. Liao, T. Lu and K. Yan, Ultrasensitive electrochemical detection of UO_2^{2+} based on DNAzyme and isothermal enzyme-free amplification, *RSC Advances*, 2016, **6**, 3960-3966.
9. D. Zhang, Z. Chen, H. Omar, L. Deng and N. M. Khashab, Colorimetric peroxidase mimetic assay for uranyl detection in sea water, *ACS Appl. Mater. Interfaces*, 2015, **7**, 4589-4594.

10. J. Wen, S. Li, Z. Huang, W. Li and X. Wang, Colorimetric detection of Cu^{2+} and UO_2^{2+} by mixed solvent effect, *Dyes. Pigments*, 2018, **152**, 67-74.
11. S. Dutta, C. Ray, S. Sarkar, M. Pradhan, Y. Negishi and T. Pal, Silver nanoparticle decorated reduced graphene oxide (rGO) nanosheet: a platform for SERS based low-level detection ofuranyl ion, *ACS Appl. Mater. Interfaces*, 2013, **5**, 8724-8732.
12. S. J. Xiao, J. Zuo, Z. Q. Zhu, Y. Z. Ouyang, X. L. Zhang, H. W. Chen and L. Zhang, Highly sensitive DNAzyme sensor for selective detection of trace uranium in ore and natural water samples, *Sensor Actuat. B-chem*, 2015, **210**, 656-660.
13. J.-X. Hou, J.-P. Gao, J. Liu, X. Jing, L.-J. Li and J.-L. Du, Highly selective and sensitive detection of Pb^{2+} and UO_2^{2+} ions based on a carboxyl-functionalized Zn(II)-MOF platform, *Dyes. Pigments*, 2019, **160**, 159-164.
14. R. Gupta, M. Sundararajan and J. S. Gamare, Ruthenium nanoparticles mediated electrocatalytic reduction of UO_2^{2+} ions for its rapid and sensitive detection in natural waters, *Anal. Chem.*, 2017, **89**, 8156-8161.
15. Z. Wang, C. Xu, Y. Lu, F. Wu, G. Ye, G. Wei, T. Sun and J. Chen, Visualization of adsorption: luminescent mesoporous silica-carbon dots composite for rapid andselective removal of U (VI) and in situ monitoring the adsorption behavior, *ACS Appl. Mater. Interfaces*, 2017, **9**, 7392-7398.
16. S. Lee, K. Y. Kim, N. Y. Lim, J. H. Jung, J. H. Lee, M. Y. Choi and J. H. Jung, Terpyridine-based complex nanofibers with Eu^{3+} as a highly selective chemical probes for UO_2^{2+}, *J. Hazard. Mater.*, 2019, **378**, 120713.
17. G. Bayramoglu and M. Y. Arica, MCM-41 silica particles grafted with polyacrylonitrile: modification in to amidoxime and carboxyl groups for enhanced uranium removal from aqueous medium, *Micropor. Mesopor. Mat*, 2016, **226**, 117-124.
18. X. Zhang, C. Jiao, J. Wang, Q. Liu, R. Li, P. Yang and M. Zhang, Removal of uranium (VI) from aqueous solutions by magnetic Schiff base: Kinetic and thermodynamic investigation, *Chem. Eng. J.*, 2012, **198-199**, 412-419.

19. M. Xu, T. Wang, P. Gao, L. Zhao, L. Zhou and D. Hua, Highly fluorescent conjugated microporous polymers for concurrent adsorption and detection of uranium, *J. Mater. Chem. A.*, 2019, **7**, 11214-11222.

20. B. Li, C. Bai, S. Zhang, X. Zhao, Y. Li, L. Wang, K. Ding, X. Shu, S. Li and L. Ma, An adaptive supramolecular organic framework for highly efficient separation of uranium via an in situ induced fit mechanism, *J. Mater. Chem. A.*, 2015, **3**, 23788-23798.

21. H. Li, Y. Li, Y. Zhou, B. Li, D. Liu and H. Liao, Efficient removal of uranium using a melamine/trimesic acid-modified hydrothermal carbon-based supramolecular organic framework, *J. Colloid Interf Sci.*, 2019, **544**, 14-24.

22. S. Huang, S. Jiang, H. Pang, T. Wen, A. M. Asiri, K. A. Alamry, A. Alsaedi, X. Wang and S. Wang, Dual functional nanocomposites of magnetic $MnFe_2O_4$ and fluorescent carbon dots for efficient U (VI) removal, *Chem. Eng. J.*, 2019, **368**, 941-950.

23. R. Wen, Y. Li, M. Zhang, X. Guo, X. Li, X. Li, J. Han, S. Hu, W. Tan, L. Ma and S. Li, Graphene-synergized 2D covalent organic framework for adsorption: A mutual promotion strategy to achieve stabilization and functionalization simultaneously, *J. Hazard. Mater.*, 2018, **358**, 273-285.

24. B. Li, Q. Sun, Y. Zhang, C. W. Abney, B. Aguila, W. Lin and S. Ma, Functionalized porous aromatic framework for efficient uranium adsorption from aqueoussolutions, *ACS Appl. Mater. Interfaces*, 2017, **9**, 12511-12517.

25. X. Liu, J. Wu, S. Zhang, C. Ding, G. Sheng, A. Alsaedi, T. Hayat, J. Li and Y. Song, Amidoxime-functionalized hollow carbon spheres for efficient removal of uranium from wastewater, *ACS Sustain Chem. Eng.*, 2019, **7**, 10800-10807.

26. Q. Sun, B. Aguila, L. D. Earl, C. W. Abney, L. Wojtas, P. K. Thallapally, and S. Ma, Covalent organic frameworks as a decorating platform foutilization and affinity enhancement of chelatingsites for radionuclide sequestration, *Adv. Mater.*, 2018, **30**, 1705479.